ISET Journal of Earthquake Technology, Paper No. 574, Vol. 59, No. 4, Dec. 2022, pp. 129-150

RESPONSE OF REINFORCED CONCRETE BUILDINGS TO EARTHQUAKE AND TSUNAMI FORCES

Akshaykumar M. Bhoi (Corresponding Author)
Department of Civil Engineering, SGGS Institute of Engineering and Technology
Nanded, Maharashtra, E mail id: *akshaybhoi@gmail.com*

Madhav P. Kadam
Department of Civil Engineering, MVPS's KBT College of Engineering
Nashik, Maharashtra, E mail id: *kadammadhavp@gmail.com*

Atul K Desai
Department of Civil Engineering
Sardar Vallabhbhai National Institute of Technology
Surat, Gujrat, E mail id: *akd@amd.svnit.ac.in*

ABSTRACT

This research investigates the complex interplay between these natural hazards and the structural response of reinforced concrete buildings. Through a meticulous analysis of four distinct structural configurations, this study offers valuable insights into the structural behavior of buildings subjected to seismic and tsunami forces. The study delves into key parameters that influence structural performance, including base shear, axial and shear forces in columns, bending moments, and storey displacement. Notably, the study identifies the columns at the forefront of structures as particularly vulnerable to tsunami impact, bearing the highest axial and shear forces. Furthermore, the presence or absence of infill walls in lower floors significantly influences the distribution of bending moments within buildings. In assessing inter-storey displacement, the study reveals that it is more pronounced below the tsunami inundation depth, demonstrating the distinct behavior of structures in response to tsunami forces.

KEYWORDS: Tsunami, Seismic Analysis, Reinforced Concrete Building

INTRODUCTION

Over the last few decades, there has been a substantial rise in the coastal population, consequently driving an upsurge in coastal development. This surge in coastal development has translated into a higher concentration of structures that are vulnerable to coastal hazards. Furthermore, contemporary residential buildings are not only more substantial in size but also possess greater intrinsic value compared to their predecessors, thereby amplifying the potential economic losses incurred during catastrophic events. To address the growing hazards and benefit from the experiences of past storms, regulatory standards governing construction in coastal regions have undergone significant enhancements over the past decade [1]–[5].

Tsunamis have emerged as a significant natural disaster in the modern era, casting doubt on their rarity. The world has seen an alarming increase in destructive tsunamis over the last two decades, each of which has had devastating effects on coastal regions around the world. For example, the 2004 Indian Ocean Tsunami, which was triggered by a massive M9.3 undersea earthquake off Sumatra's western coast, unleashed waves as tall as 30 metres, killing 230,000 people in 14 countries and destroying 96,000 structures in Sri Lanka [6]–[10]. Another tragic example is the March 2011 East Japan tsunami, which was caused by the M9.0 Tohoku earthquake and killed over 15,000 people. The tsunami destroyed 121,739 structures and partially damaged an additional 279,088, including critical infrastructure such as nuclear power plants, as well as destroying over 4,000 roads and bridges [11]. Since 1990, fourteen tsunamis have caused economic losses in excess of USD 1 million, with the 2011 Japan tsunami topping the list with damages totalling USD 220 billion [12]. These records show that tsunamis pose a significant threat to coastal communities worldwide, necessitating the urgent development of robust methodologies and models to assess their impact on buildings and infrastructure. These tools are critical for risk management, urban planning, and building design in high-risk areas. P. Kodanda Rama Rao et. al. [13] conducted a comprehensive analysis on a shelter building, exploring various structural configurations and conducting a comparative assessment of their responses. The study involved the determination of seismic forces in accordance with the IS 1893(2002) [14] seismic code, while hydrodynamic forces were evaluated using FEMA's Coastal Construction Manual (CCM) [15]–[17]. One noteworthy contribution of the paper is the development of a valuable guideline pertaining to the building's height. The authors proposed a critical height (hc) at which earthquake forces and tsunami forces are of equal magnitude. Below this height, earthquake forces dominate, whereas above hc, tsunami forces take precedence. This guideline offers practical insights for future design considerations, potentially improving the effectiveness and resilience of coastal structures. P. Lukkunaprasit et al. [18] emphasized the significance of openings in Reinforced Concrete (RC) buildings with masonry infill panels for cost-effective and safe vertical evacuation shelter design against tsunamis. Their findings revealed that openings had a negligible influence on peak pressures on the model's front face. Nonetheless, models with 25% and 50% openings reduced tsunami forces by approximately 15% and 30%, respectively, compared to those without openings. This highlights the distinct advantage of incorporating openings in mitigating tsunamis' impact on such structures. Ioan Nistor, Dan Palermo et al [19] conducted an extensive research program aimed at understanding tsunami-induced forces on coastal infrastructure. Their primary goal was to elucidate the complex hydrodynamic mechanisms governing the impact and extreme loading experienced by shorefront buildings in tsunami-prone coastal areas. They sought to accurately quantify these loads and propose new design formulations to enhance structural resilience in such regions.

Y. Nakano's [20] study highlights the crucial role of tsunami shelters in reducing casualties from earthquake-induced killer waves. While practical design formulas for calculating tsunami loads on shelters have been proposed, they primarily rely on laboratory tests with scaled models rather than damage observations. The study's findings suggest that the design tsunami loads recommended in guidelines are generally effective in preventing severe damage.

Extensive post-disaster investigations conducted by FEMA and various other reputable organizations [15]–[17] have consistently underscored the importance of proper siting, meticulous design, and meticulous construction in ensuring the robust performance of coastal residential buildings. This crucial aspect significantly contributes to mitigating physical and financial losses within coastal communities. To enhance the resilience of coastal regions, there is a pressing need to advance our understanding of two critical elements: firstly, the accurate assessment of lateral resistance in onshore structures against tsunami-induced forces, and secondly, the precise quantification of the impact forces exerted by waterborne debris. Attention to detail in the structural design of components exposed to these forces is imperative.

In the aftermath of the devastating Indian Ocean Tsunami of December 2004, reconnaissance missions vividly illustrated the potential for severe damage or even collapse of reinforced concrete structures [6]–[8]. Consequently, there has been a pronounced shift towards prioritizing research efforts aimed at stimulating the generation, propagation, and run-up of tsunami waves among scientists in the affected coastal regions. Notably, wooden structures often succumb to immediate collapse or flotation during tsunamis, while the substantial weight of reinforced concrete structures typically anchors them in place. However, the March 2011 tsunami in Japan underscored that the immense pressure exerted by tsunami waves can result in the wholesale failure of reinforced concrete structures. Thus, the meticulous analysis and design of reinforced concrete structures in tsunami-prone areas assume paramount significance.

In the realm of structural vulnerability assessment, several notable studies have contributed valuable insights. Park et al. [17] pioneered the development of fragility curves for a two-story wooden building, subjecting it to sequential earthquake and tsunami loading. Their analysis adhered to the FEMA P-646 [17] guidelines for tsunami loads. Latcharote and Kai [21], on the other hand, delved into the behavior of a seven-story RC wall-frame building, employing both Earthquake Dynamic (EDY) and subsequent Constant-Depth Push Over (CDPO) analyses to evaluate its response to tsunami loading. Petrone et al. [22] extended the exploration by crafting fragility functions for a 5-story RC moment-resisting frame building. Their dynamic analysis encompassed both earthquake and tsunami loading, specifically focusing on the 2011 Tohoku earthquake. Notably, their findings underscored that the antecedent earthquake did not significantly influence the subsequent tsunami response. This observation stemmed from the distinct failure mechanisms associated with each hazard, namely flexure for seismic forces and shear for tsunami loads. Moreover, their work emphasized the imperative of designing basal columns to withstand tsunami-induced shear actions. Tagle et al. [23] undertook an insightful assessment of a typical Chilean modern RC wall building. Utilizing the nonlinear finite element method (FEM), they conducted simulations, aligning with the double pushover approach. Their meticulous work contributed to a deeper understanding of the structural behavior in the face of earthquake and tsunami forces. Recent investigations by Rossetto et al. [24], [25] expanded on the analysis of structures subjected to seismic and tsunami actions. In their research, a Japanese tsunami evacuation building served as a pivotal case study, and diverse dynamic and static analytical methods were employed to assess the structure's response to both earthquake and tsunami loading phases. These methods encompassed well-established earthquake analysis techniques, such as nonlinear dynamic response-history analysis (DY) and nonlinear static pushover analysis (PO), as well as innovative approaches tailored to tsunami loading, including nonlinear response history analysis, Constant Depth Push Over analyses (CDPO), and Variable Depth Push Over analyses (VDPO) [26]. This multifaceted exploration enhanced our understanding of structural behavior in the face of dual hazards.

Traditionally, the primary approach for mitigating earthquake-related fatalities has revolved around enhancing building seismic design codes. Conversely, to mitigate tsunami-induced casualties, the prevailing strategy has been the development and construction of horizontal tsunami evacuation plans in elevated urban areas. However, in instances where near-field tsunamis are a pressing threat, the intricate urban topography may impede timely access to safety zones [26]. Therefore, the adoption of vertical evacuation measures emerges as a viable option for safeguarding lives. Several countries, including Japan, the United States, and Indonesia, have implemented various forms of vertical evacuation shelters, which have demonstrated notable success in past disaster events [26]. These initiatives represent crucial endeavors in disaster risk reduction.

The objective of this study is to conduct a comprehensive investigation into the behavior of reinforced concrete framed structures under the combined influence of seismic and tsunami-induced hydrodynamic loads. Specifically, this study aims to identify and analyze the key factors and considerations that need to be incorporated into the design process for such structures. To achieve these objectives, the research involves the analysis of four structural configurations in accordance with Indian standards (IS:1893-2016) [14] for seismic design and hydrodynamic load calculations from relevant equations [8], [15], [16]. The performance assessment of these structures is carried out through non-linear response spectrum analysis.

METHODOLOGY

This study is structured into distinct phases. During the initial phase, we developed detailed models of reinforced concrete frames using SAP 2000 software with four distinct structural configurations. By examining and contrasting the structural behaviour under these configurations, valuable insights were gained to inform the design process.

BUILDING CONFIGURATION

The building is analysed with its location in seismic zones II, III, VI, and V as delineated in the Indian seismic zone map. The foundation type employed for this study is the isolated footing design. To optimize the building's orientation with respect to the approaching tsunami wave, we oriented the shorter side of the structure parallel to the shoreline, thereby minimizing the frontal area facing the tsunami wave. To investigate the effect of earthquake and tsunami forces on a ground-plus-four-story reinforced concrete building, the following four configurations were considered.

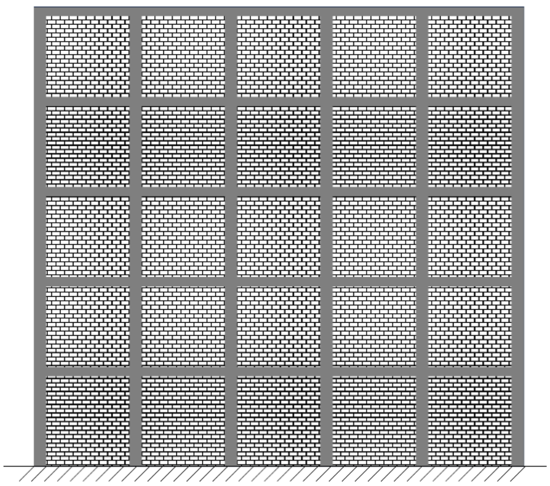

Fig. 1 Configuration 1

Configuration 1: All storey with inner and outer infill walls.

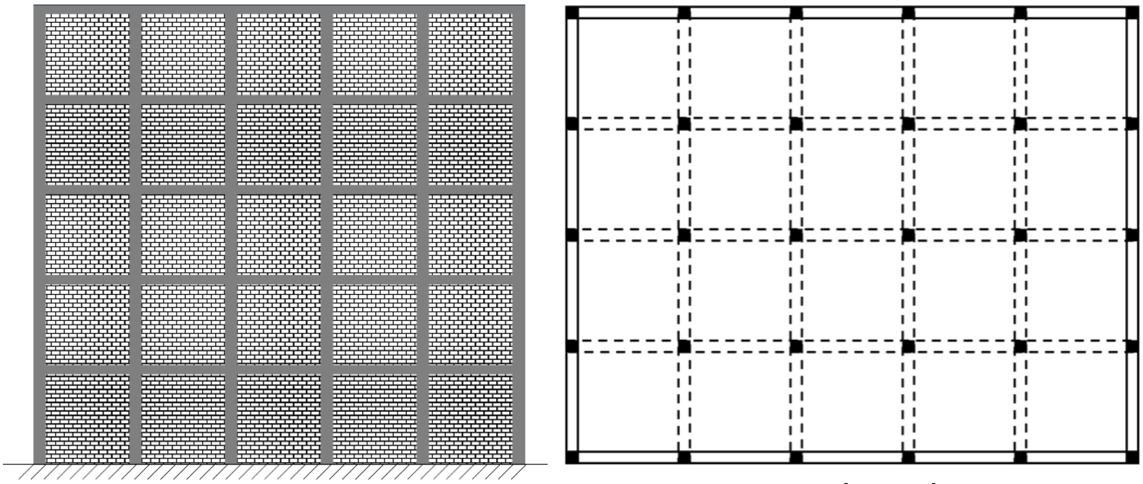

(a) Elevation **(b) Plan for 3rd and 4th Storey**

Fig. 2 Configuration 2

Configuration 2: Third and fourth storey with only outer infill walls, whereas all other storey with inner and outer infill walls.

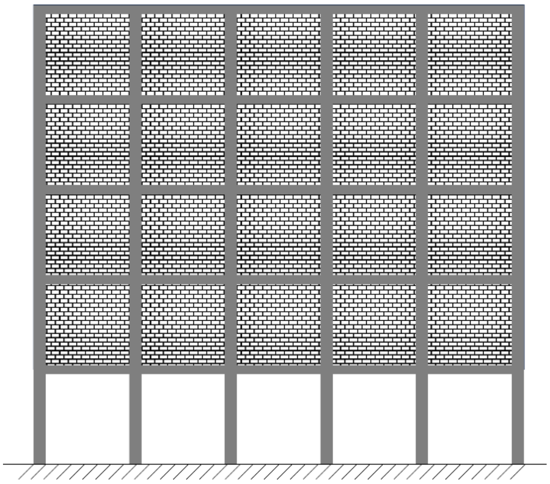

Fig. 3 Configuration 3

Configuration 3: The ground floor is devoid of infill walls, whereas all other floors feature inner and outer infill walls.

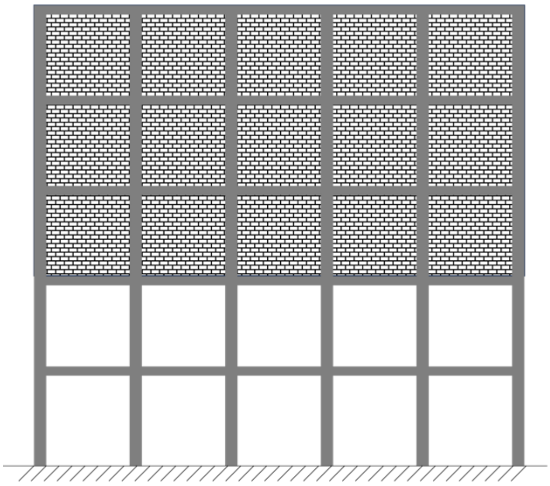

Fig. 4 Configuration 4

Configuration 4: The ground and first floors are devoid of infill walls, whereas all other floors feature inner and outer infill walls.

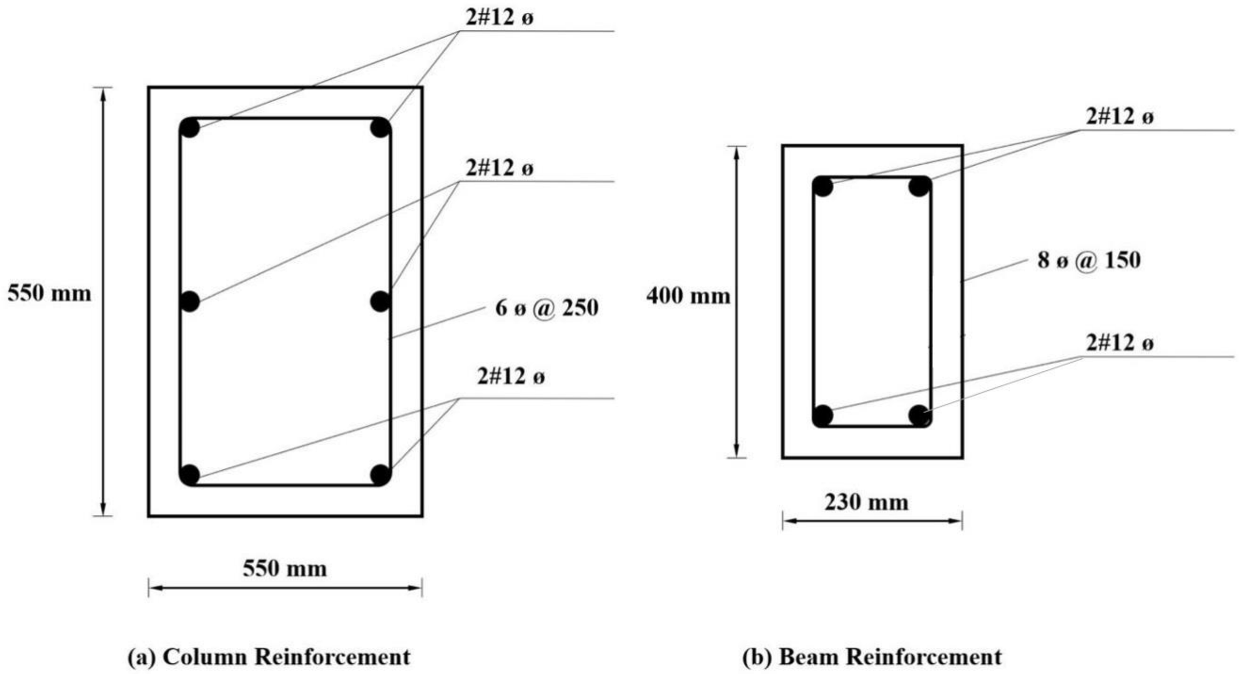

Fig. 5 Reinforcement details of columns and beams

TSUNAMI INDUCED DESIGN FORCES

The existing structural design codes offer minimal guidance on tsunami-induced forces and their impact on coastal construction. To address this gap, a set of generalized equations has been adopted by synthesizing information from current building codes and published literature. These equations encompass various aspects of tsunamis, including flooding, breaking waves, and associated forces such as lateral hydrostatic force, buoyant force, hydrodynamic force, surge force, impact force, and breaking wave forces. In this article, we focus on elucidating the components of tsunami-induced hydrodynamic drag and impulsive forces, providing concise descriptions, and presenting analytical and empirical formulas for calculating each component. Furthermore, we delve into the loading combinations for these force components.

1. Hydrodynamic Drag Force

Hydrodynamic forces manifest when water flows around a building at elevated speeds above ground level, primarily as lateral forces arising from the impact and drag of the moving water mass around the structure. These resultant forces typically act at approximately half the distance from the design still water level.

In the context of a tsunami advancing inland at a substantial velocity, structures are exposed to hydrodynamic forces generated by drag. Currently, there exist variations in estimating the magnitude of these hydrodynamic forces. Equation 1 presents the general expression for this force. Different design codes employ this expression but employ varying drag coefficient values (CD). For instance, circular piles are recommended to have CD values of 1.0 by CCH and 1.2 by FEMA 55. In the case of rectangular piles, both FEMA 55 CCH suggest a drag coefficient of 2.0. [15]–[17]

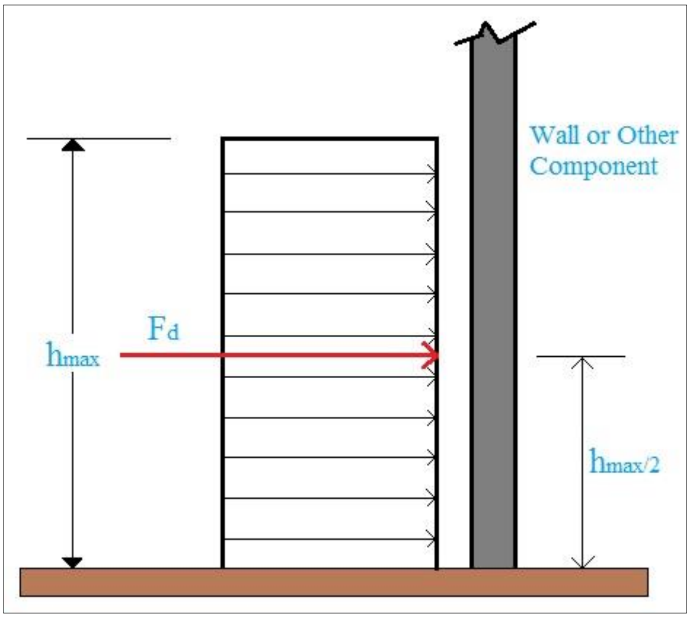

Fig. 6 Hydrodynamic drag force distribution

FEMA & CCH $$F_D = \frac{\rho C_D A}{2} u^2 \quad (1)$$

Where,

F_D = Total drag force acting in the direction of flow (kN),
C_D = Drag coefficient.
A = Projected area of the body normal to the flow direction (m^2) and
u = Bore velocity (m/s).

2. Tsunami-bore Velocity

Prior research has focused on the estimation of hydrodynamic drag and impulsive forces exerted on structures by tsunami bores. These forces exhibit a strong dependence on bore velocity, with the hydrodynamic drag being proportional to the square of velocity and the impulsive force being linearly proportional. Consequently, uncertainties in velocity estimations can lead to significant variations in the magnitude of these forces.

During major tsunami inundations, there can be considerable variations in tsunami-bore velocity and direction. Present estimates of velocity tend to be conservative, assuming high flow velocities impacting structures at normal angles. Additionally, current design codes lack consideration for factors such as run-up, backwash, and velocity direction.

While a general equation for hydrodynamic force has garnered consensus, researchers have proposed various empirical coefficients, contributing to variations in force estimations. Equation 2 outlines the general form of bore velocity, highlighting its relevance in this context.

$$u = C\sqrt{gd_s} \quad (2)$$

Where,

u = Bore velocity (m/s),
d_s = Inundation depth (m) and
C = Constant coefficient.

Multiple formulations have been put forth by different sources, including FEMA 55 to estimate tsunami bore velocity based on inundation depth The velocities computed using FEMA 55 serve as lower and upper bounds, respectively.

3. Impulsive Force

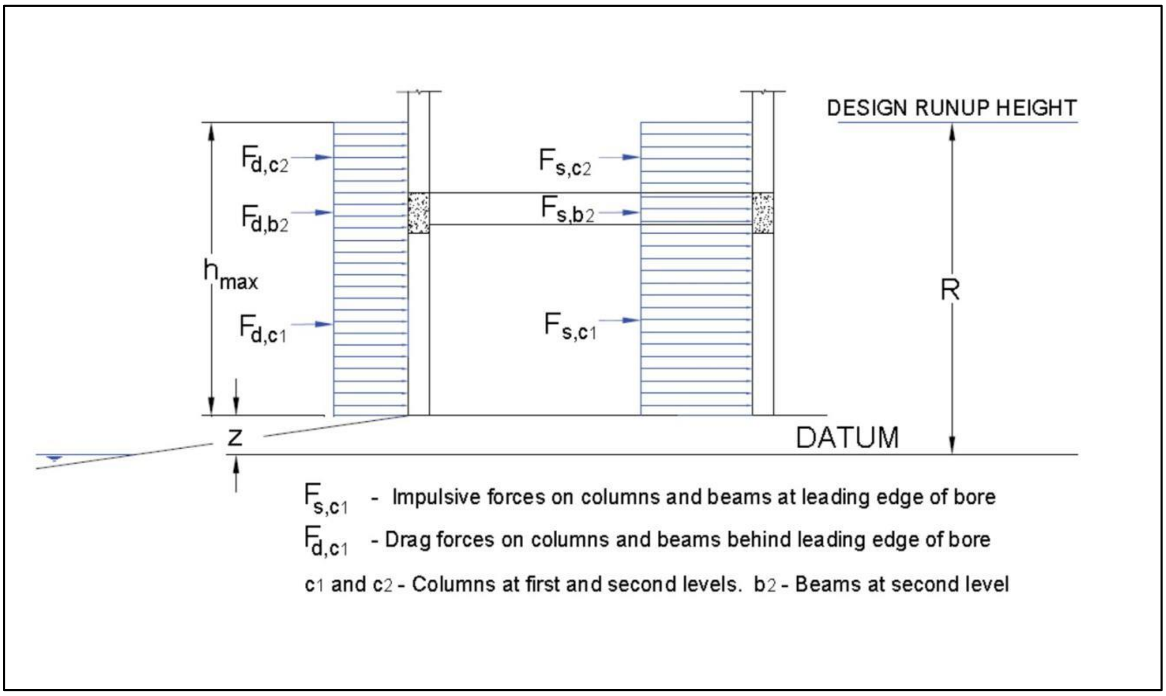

Fig. 7 Hydrodynamic drag and impulsive forces on components of a building subjected to inundation by tsunami bore

Impulsive forces result from the initial impact of the advancing surge of water against a structure. To err on the side of caution, it is advisable to consider the impulsive force as 1.5 times the hydrodynamic drag force, as expressed in Equation 3.

$$F_s = 1.5F_D \tag{3}$$

These impulsive forces predominantly affect structural elements located at the forefront of the tsunami bore, whereas hydrodynamic drag forces influence all elements that have been overtaken by the bore's leading edge, as illustrated in Figure 7.

3. Tsunami load combinations

In the study conducted by D. Palermo and I. Nistor in 2008 [27], the characterization of tsunami loads was undertaken with a focus on their extreme nature, leading to the identification of three distinct load cases for analytical purposes. The first load case exclusively incorporates Tsunami (T) and Dead (D) loads. The second load case expands the scope to include additional concurrent loads, such as Live (L) and Snow (S) loads. Following load combinations for the Tsunami forces are considered in the present study.

i) T + 1.0 DL

ii) T + 1.0 DL + 0.5 LL

EARTHQUAKE LOAD ANALYSIS

In this research study, the calculation of earthquake loads was performed using a response spectrum analysis method in accordance with the guidelines outlined in the Indian Standard IS 1893-Part 1-2016[14]. The earthquake load combinations were chosen in accordance with the prescribed guidelines as stipulated in the Indian Standard IS 1893-Part 1-2016. In this study, the contribution of elastic in-plane stiffness from unreinforced masonry infill is analogously represented as an equivalent compression strut. This strut possesses identical thickness and modulus of elasticity to the infill panel it represents. Furthermore, the determination of the equivalent width (w_{ds}) adhered to the guidelines specified in the Indian Standard IS 1893-Part 1-2016.

The width is given by

$$w_{ds} = 0.175{\alpha_h}^{-0.4}L_{ds} \tag{4}$$

Where,

$$\alpha_h = h\left\{\sqrt[4]{\frac{E_m t \sin 2\theta}{4E_f I_c h}}\right\} \tag{5}$$

where E_m and E_f are the modulii of elasticity of the materials of the unreinforced masonry infill and reinforced concrete moment resisting frame, I_c the moment of inertia of the adjoining column, t the thickness of the infill wall, and θ the angle of the diagonal strut with the horizontal.

ANALYSIS METHOD AND MODELLING

This study employs numerical modeling techniques utilizing the SAP2000 software. In our study, we focused on a G+4-story reinforced concrete (RC) frame building, positioned in a region susceptible to tsunami inundation. The building featured floor plan dimensions measuring 16 meters by 20 meters, with a inter storey height of 4m. It comprised six distinct resisting frames with 4 bays spaced at 4-meter intervals, as illustrated in Figure 8. These frames incorporated columns and beams with cross-sectional details depicted in Figure 5. To determine the structural loads, we followed the stipulations outlined in the Indian Standard BIS 875-Part2 (2003) for live loads and referenced the Indian Standard BIS 1893-2016 for earthquake forces, considering a soft soil type. For tsunami forces, we adhered to the FEMA P646 guidelines, assuming inundation depth of 3, 6, and 9 m. M25 grade of concrete and Fe 415 steel was considered. Additionally, in line with the recommendations put forth by Petrone et al. [11], we designed transverse reinforcements for the columns to mitigate the risk of tsunami-induced shear failure. Our investigation delved into the structural response of the building under the influence of earthquake and tsunami loads, employing nonlinear dynamic analyses. These analyses encompassed a total of four distinct configurations under consideration based on the presence of infill walls. The procedural steps undertaken in this study are outlined as follows.

1. **Structural Modelling**: The initial phase involves the creation of a structural model for a ground-plus-four-floor building, meticulously aligning it with the planned floor layout, as determined by the authors' estimates.

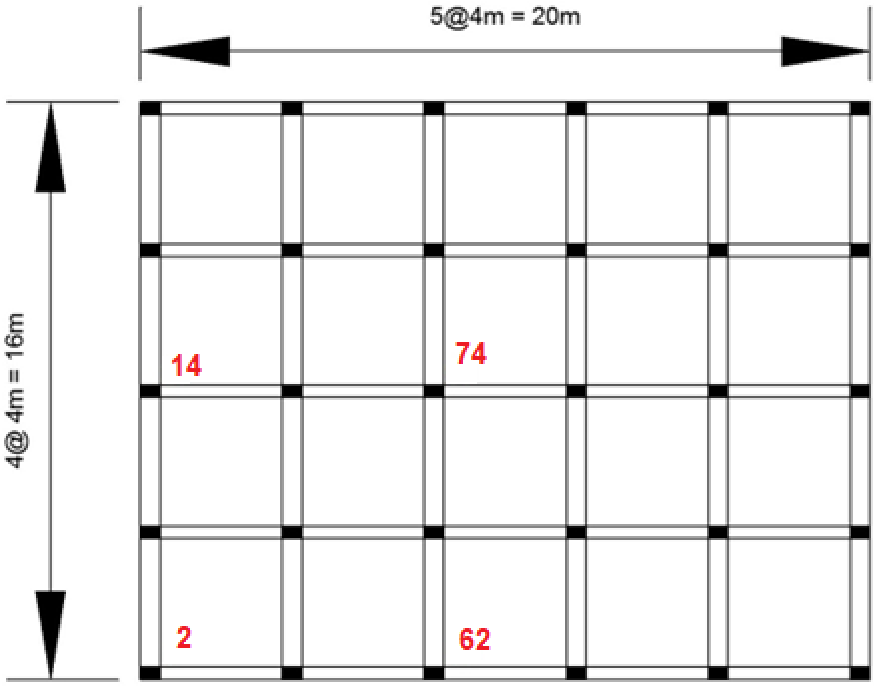

Fig. 8 Plan for Ground+4 storey building showing joints considered for comparing displacement

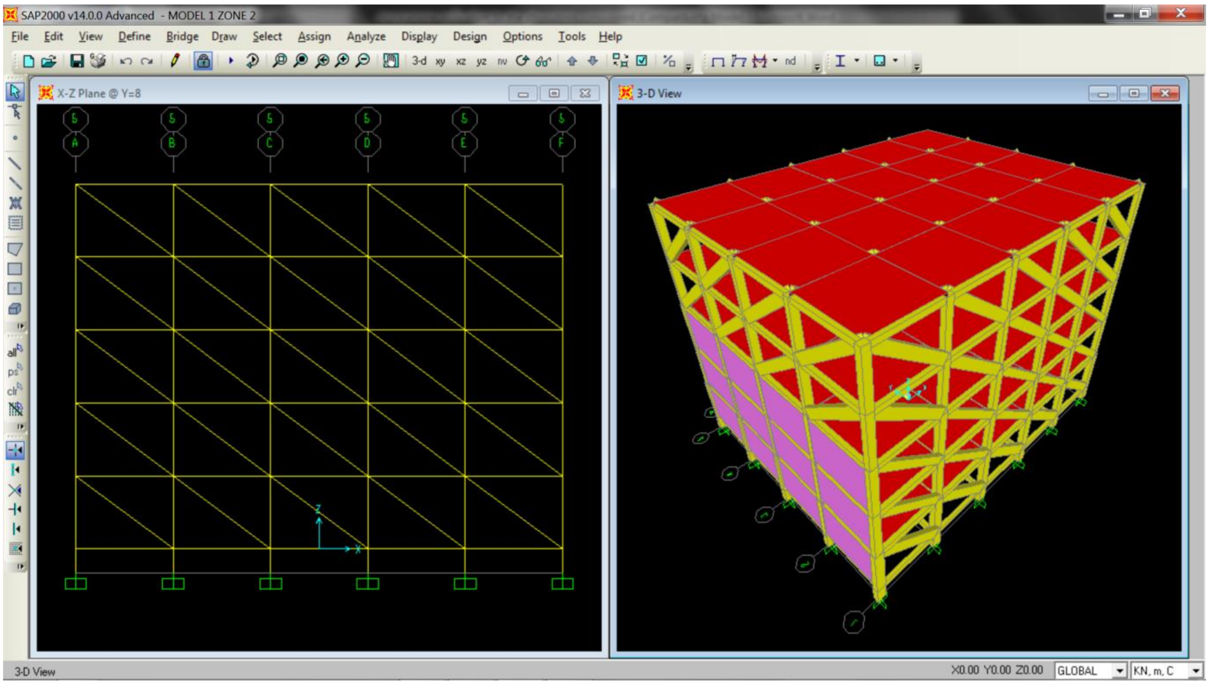

Fig. 9 Modelling in SAP2000

2. **Earthquake Load Assessment**: Subsequently, the study entails evaluating earthquake loads and assessing the resultant base shear, joint displacement, axial force, bending moment, shear force, and storey drift, ensuring compliance with predefined requirements before subjecting the structure to tsunami loads in later stages. The study focuses on a planned reinforced concrete moment frame building characterized by its utilization of an ordinary moment resisting frame system, all of which is situated on a soft ground foundation. Plans illustrated in Figure 9. In this study, we represent the contribution of elastic in-plane stiffness from unreinforced masonry infill using an analogous representation known as an equivalent compression strut, as elaborated in Section 2.3.
3. **Tsunami Load Analysis**: The analysis of tsunami loads incorporates the calculation of tsunami forces, following the loading combination guidelines outlined in FEMA P646 [17]. This assessment extends to structural analyses conducted under varying tsunami wave heights of 3m, 6m, and 9m. The study then examines the impact of both earthquake and tsunami loads on the structural behaviour, considering internal forces, drift, and drift ratios. The comparative results are visually presented through graphs. In this study, we consider a beach slope of 1 in 50 and calculate inundation depths (h_{max}) corresponding to various tsunami heights. It is essential to note that inundation depth and the flow velocity of a tsunami wave represent critical parameters when evaluating the external forces acting on structures. The hydrodynamic drag force is expressed as directly proportional to the square of the flow velocity and the projected area of the structure. To determine the design value of $(hu^2)_{max}$ for a specific location, we utilize 10, and subsequently, we obtain the corresponding drag force associated with it.

$$(hu^2)_{max} = gR^2\left[0.125 - 0.235\left(\frac{z}{R}\right) + 0.11\left(\frac{z}{R}\right)^2\right] \tag{6}$$

Where,

R – Maximum run up height of tsunami above shore line
Z – Height of location point of the structure above shore line
h_{max} - Maximum Inundation Depth above base of the structure
u – Tsunami wave velocity approaching the structure
ρ - Mass density of sea water
b - Breadth of exposed column/wall member

Finally, drawing from the analysis outcomes, the study formulates conclusive findings and provides valuable recommendations for further consideration.

RESULTS AND DISCUSSIONS

As previously stated, various structural configurations were assessed under earthquake conditions and tsunami-induced hydrodynamic forces, all under the assumption of a fixed base. The responses were quantified in terms of base shear, joint displacement, axial force, bending moment, shear force, and storey drift for different earthquake and tsunami load levels. In pursuit of comparative analysis, we have identified Joint numbers 7, 21, 77, and 91, as illustrated in Figure 8. Simultaneously, we have designated the corresponding columns (numbers 2, 14, 62, and 74) for the assessment of member forces, encompassing axial force, shear force, and bending moment. The findings have been visualized through graphical plots and are subsequently discussed.

BASE SHEAR

The impact of earthquakes and tsunamis on the base shear of a reinforced concrete building constitutes a pivotal element within the realm of structural analysis and design. Tsunamis, in particular, introduce distinctive challenges due to their extended loading duration, which can yield substantial lateral forces on the building's foundation. Furthermore, the base shear during a tsunami event is influenced by various factors, including the building's structural layout, the presence of openings, the depth of inundation, and the flow velocity of the tsunami waves. Notably, the drag and impact forces exerted by tsunami waves also contribute significantly to the overall base shear. The base shear on the different structural configurations due to earthquake and tsunami loading is depicted in the Figure 10. In all the structural configurations studies, the base shear remains relatively low when subjected to a tsunami height of 3 meters, comparable to what is typically experienced in seismic zone 2. However, as the tsunami height increases to 6 meters and 9 meters, the base shear experiences a substantial surge and becomes comparable to the forces observed during earthquakes in zones 4 and 5. It's worth noting that the highest base shear values, induced by both earthquake and tsunami forces, were consistently observed in structural configuration 1. This configuration bears the highest seismic weight and presents the largest frontal area exposed to tsunami waves. Conversely, the lowest base shear values, for both earthquake and tsunami forces, were consistently associated with structural configuration 4, characterized by the lowest seismic weight and the smallest frontal area exposed to tsunami waves.

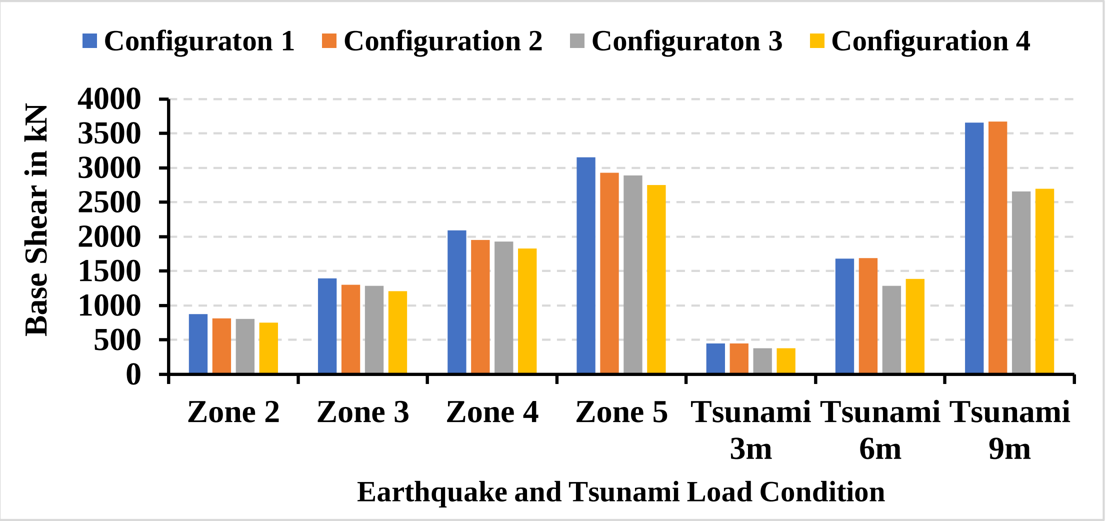

Fig. 10 Base shear due to Earthquake and Tsunami loads

AXIAL FORCE IN THE COLUMNS

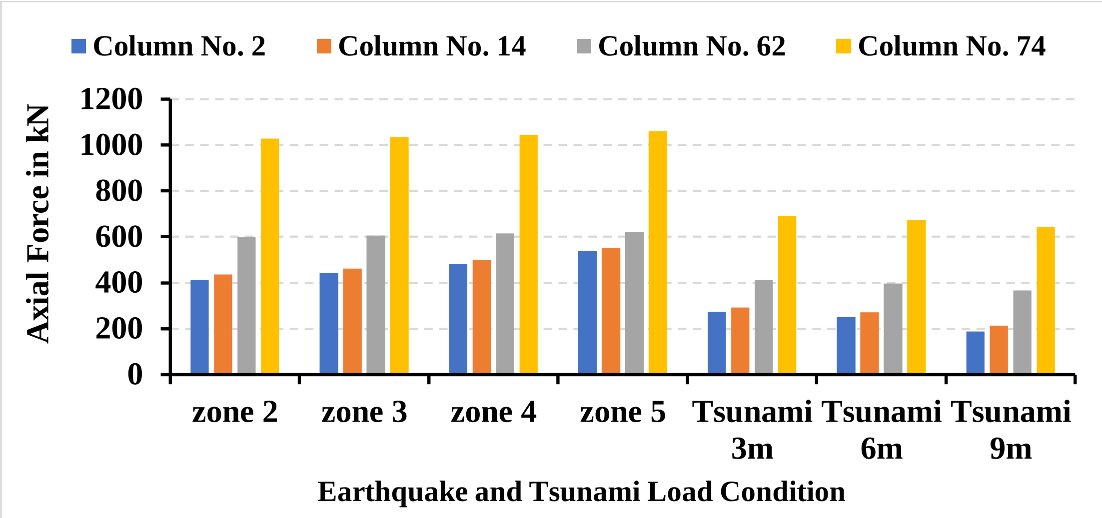

Fig. 11 Axial forces in the columns due to earthquake and Tsunami loads for configuration 1

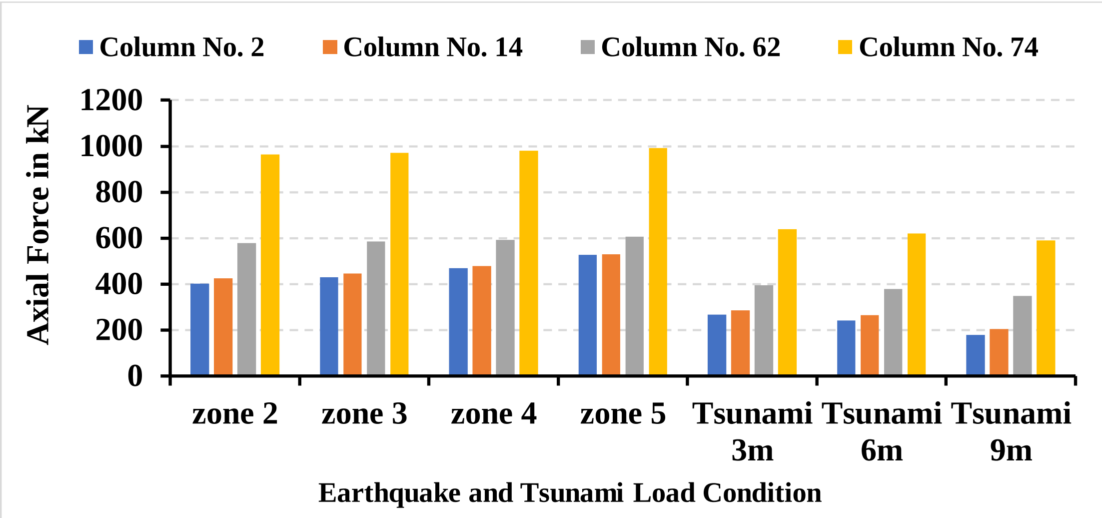

Fig. 12 Axial forces in the columns due to earthquake and Tsunami loads for configuration 2

The axial forces developed in the columns under consideration due to the effect of earthquake and tsunami loads are depicted in Figure 11, Figure 12, Figure 13, and Figure 14 respectively for structural configuration 1, 2, 3, and 4. The purpose of the evaluation on the comparison of maximum internal forces on column in terms of the different structural configurations is to find out how the structure behaves at each column position when earthquake and tsunami loads are applied. The column with the highest axial force under earthquake loads is column 74. This can be attributed to the greater axial load resulting from the combined effect of dead load (DL) and live load (LL) when compared to columns 2, 14, and 62. For the similar reason the axial fore in column 62 was second to the axial force in column 74. This phenomenon stems from the substantial lateral force experienced by the front column, which was directly impacted by the tsunami inundation. This impact created a leveraged effect within the structure, leading to an upward force on the front column. Consequently, the interior columns experienced compressive forces, thereby amplifying the axial force within these interior columns. It's essential to note that these findings are in alignment with [28], which offers valuable insights into similar phenomena. Additionally, column 62 exhibited the second-highest axial force, for analogous reasons to column 74, underlining the critical role of the tsunami impact on structural responses.

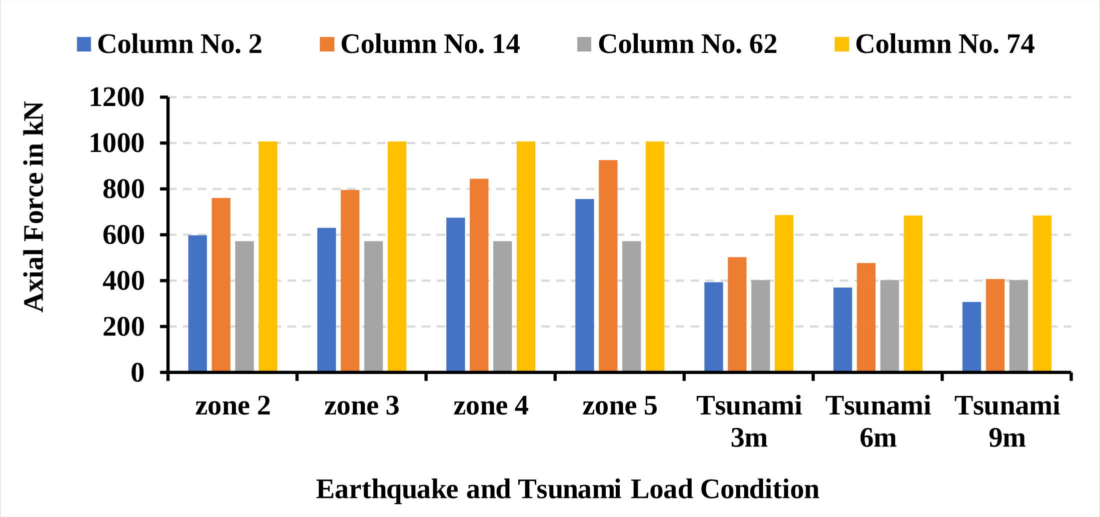

Fig. 13 Axial forces in the columns due to earthquake and Tsunami loads for configuration 3

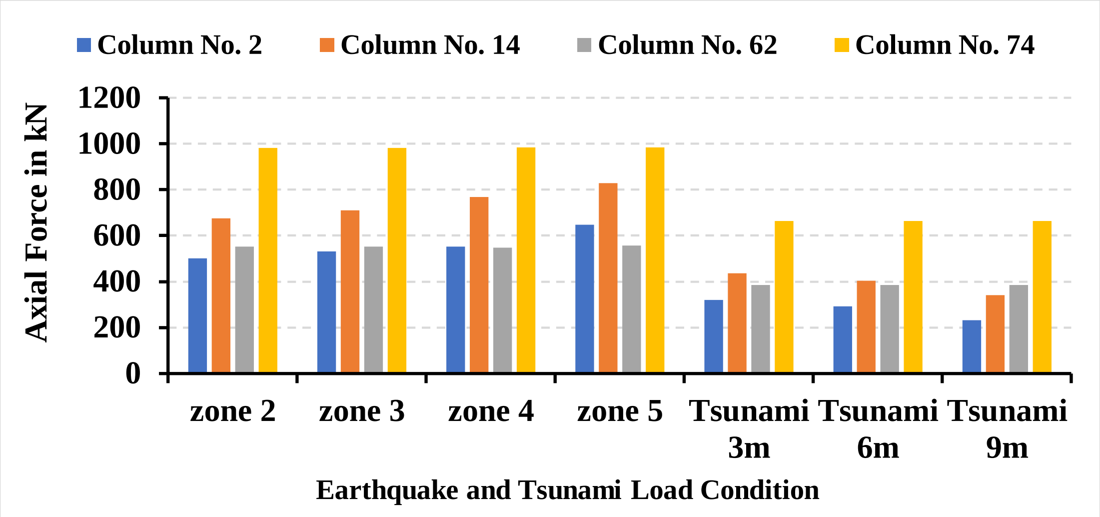

Fig. 14 Axial forces in the columns due to earthquake and Tsunami loads for configuration 4

SHEAR FORCE IN THE COLUMNS

Figures 15, 16, 17, and 18 serve as visual representations depicting the shear forces arising within the columns under investigation, originating from both earthquake and tsunami loads. It is noteworthy that a consistent pattern emerges across all structural configurations: the columns experiencing the highest shear forces induced by earthquake loads are consistently identified as columns 62 and 74. This intriguing phenomenon finds its explanation in the transmission of lateral loads from the front-positioned columns, ultimately leading to the column situated at the extreme rear of the structure bearing the brunt of the shear force. In the case of structural configurations 1 and 2, the scenario shifts when we consider the shear forces attributed to tsunami forces. Here, columns 2 and 14 emerge as the points of interest, bearing the highest shear forces. This outcome stems from the direct collision load acting upon the front-positioned columns, leading to an increased shear force concentration in these specific columns. However, when we shift our focus to structural configurations 3 and 4, a different narrative unfolds. In these configurations, the absence of infill walls on the lower floors plays a pivotal role. As a result, columns 62 and 74 are seen to exhibit their maximum shear forces. This distinctive observation highlights the significance of architectural details, such as infill walls, in governing the distribution of shear forces within a structure when subjected to tsunami loads.

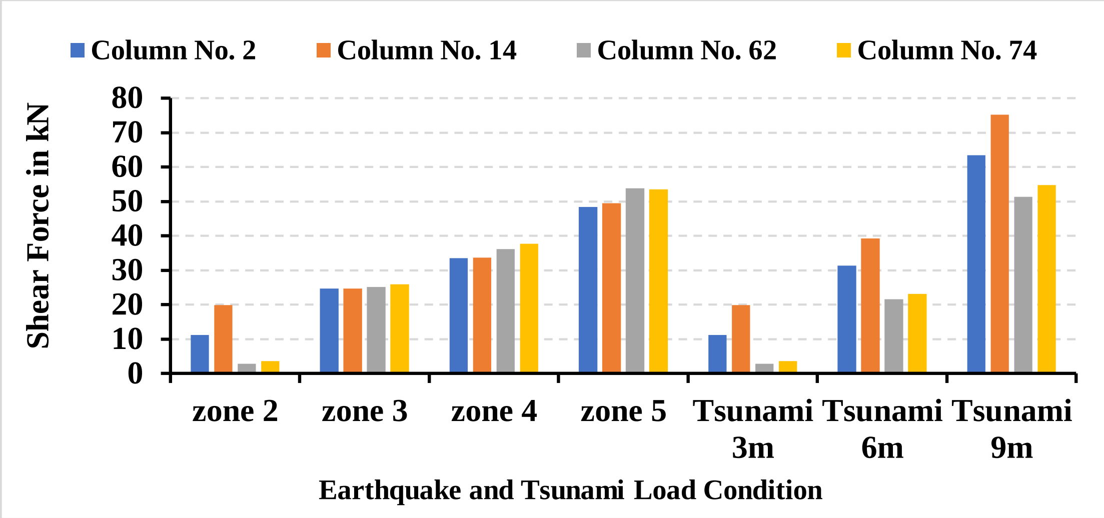

Fig. 15 Shear forces in the columns due to earthquake and Tsunami loads for configuration 1

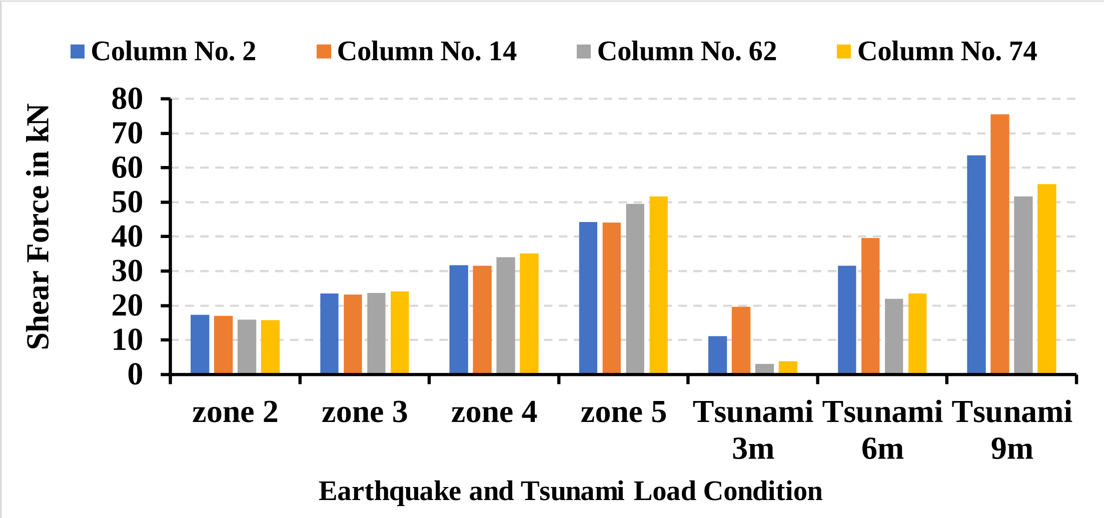

Fig. 16 Shear forces in the columns due to earthquake and Tsunami loads for configuration 2

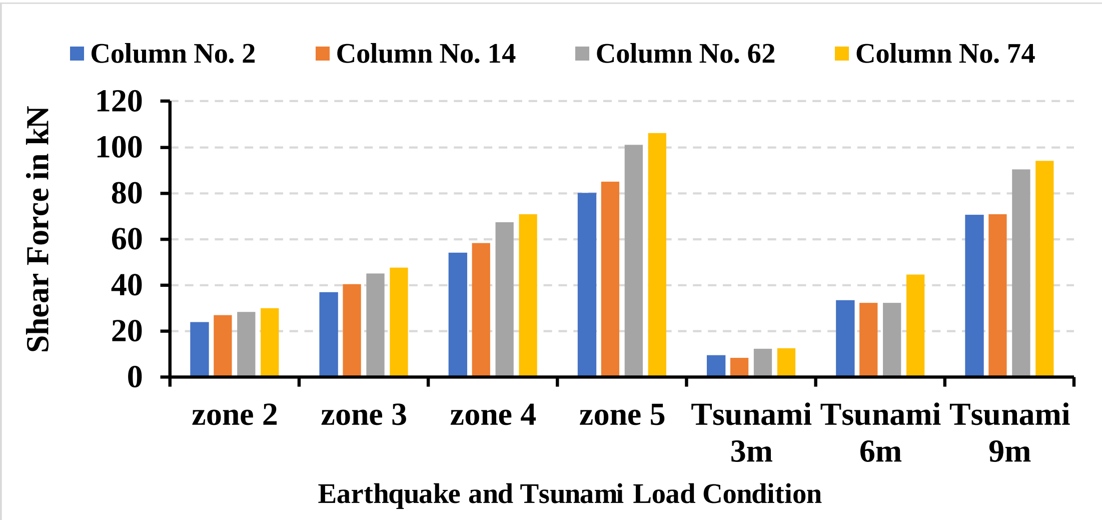

Fig. 17 Shear forces in the columns due to earthquake and Tsunami loads for configuration 3

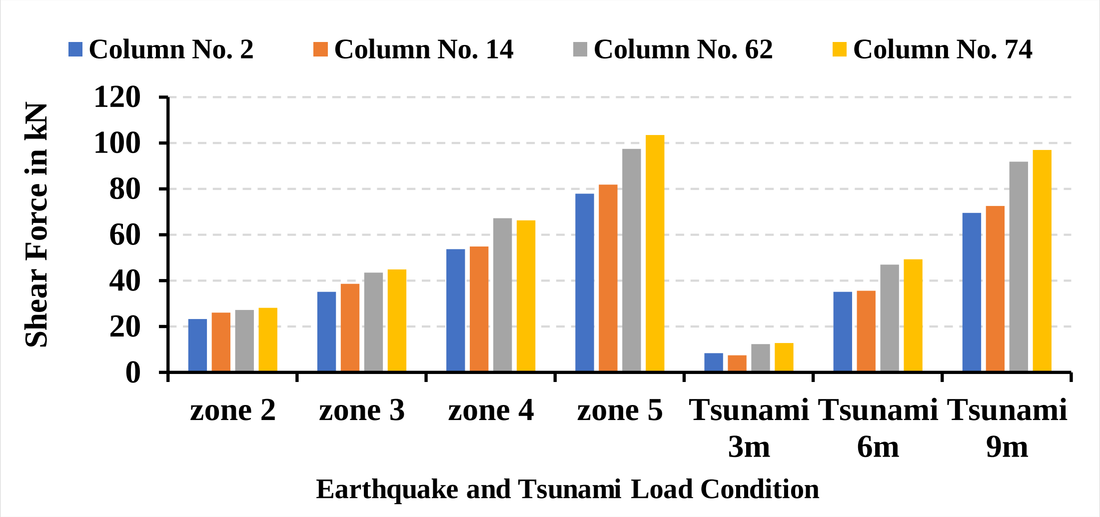

Fig. 18 Shear forces in the columns due to earthquake and Tsunami loads for configuration 4

BENDING MOMENT IN THE COLUMN

Figures 19, 20, 21, and 22 present a comprehensive visualization of the bending moments that have developed within the columns under scrutiny, stemming from both seismic and tsunami loads. These figures encapsulate a crucial aspect of the structural response to external forces and provide valuable insights into the structural behavior during these extreme events. Regarding the response to earthquake forces, a consistent trend emerges across all structural configurations. The bending moments induced by seismic loading exhibit a relatively uniform distribution among the columns under consideration. This uniformity can be attributed to the symmetric nature of the structure, where the layout and loading are balanced and evenly distributed. However, an intriguing observation emerges when examining configurations with voids or open spaces in the lower floors. In such instances, the values of the bending moments tend to be notably higher. This intriguing phenomenon can be attributed to variations in stiffness within the building. Turning our attention to the impact of tsunami forces on the structural response, a similar pattern emerges. Structural configurations 1 and 2 display lower bending moments when compared to configurations 3 and 4. In this context, a significant determinant is the presence or absence of infill walls on the lower floors of the structures. The introduction of infill walls enhances the overall structural stiffness, leading to a notable influence on the distribution of bending moments within the building. Consequently, configurations 3 and 4, characterized by a lack of infill walls on the lower levels, demonstrate elevated bending moments when subjected to tsunami forces. These findings highlight the intricate interplay between structural design, the dispersion of stiffness throughout the building, and the resultant response to external forces. They underscore the critical importance of factoring in the existence or absence of infill walls on lower floors when evaluating how bending moments are distributed in reinforced concrete structures exposed to the combined challenges of seismic and tsunami loading. Such insights are invaluable in enhancing our understanding of structural behavior and can inform more resilient design practices in regions prone to seismic and tsunami events.

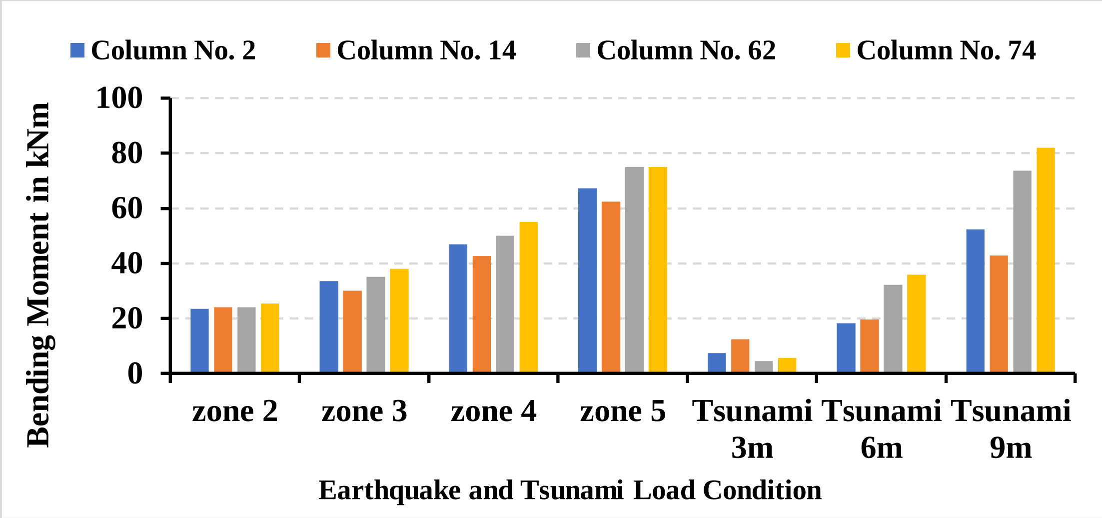

Fig. 19 Bending Moment in the columns due to earthquake and Tsunami loads for configuration 1

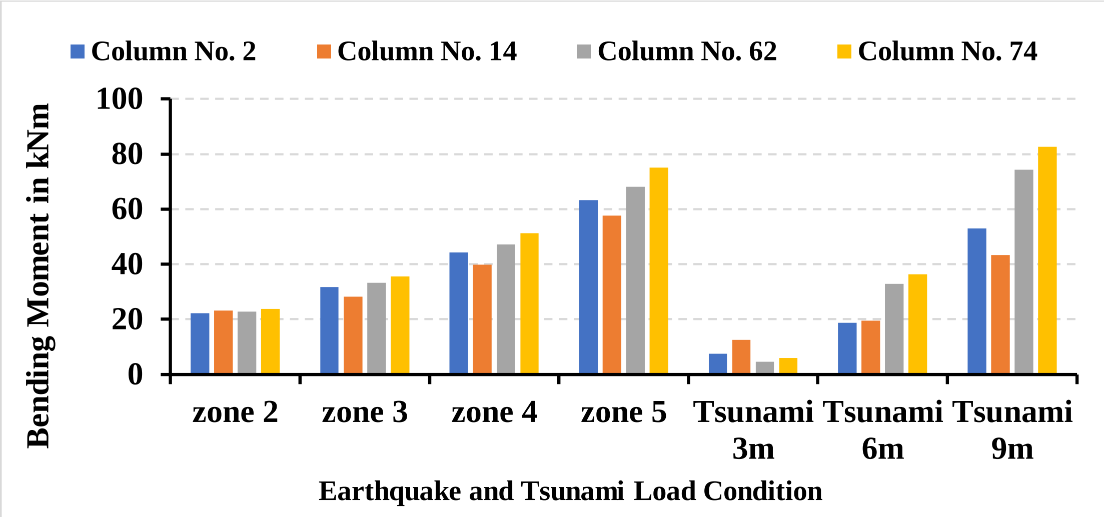

Fig. 10 Bending Moment in the columns due to earthquake and Tsunami loads for configuration 2

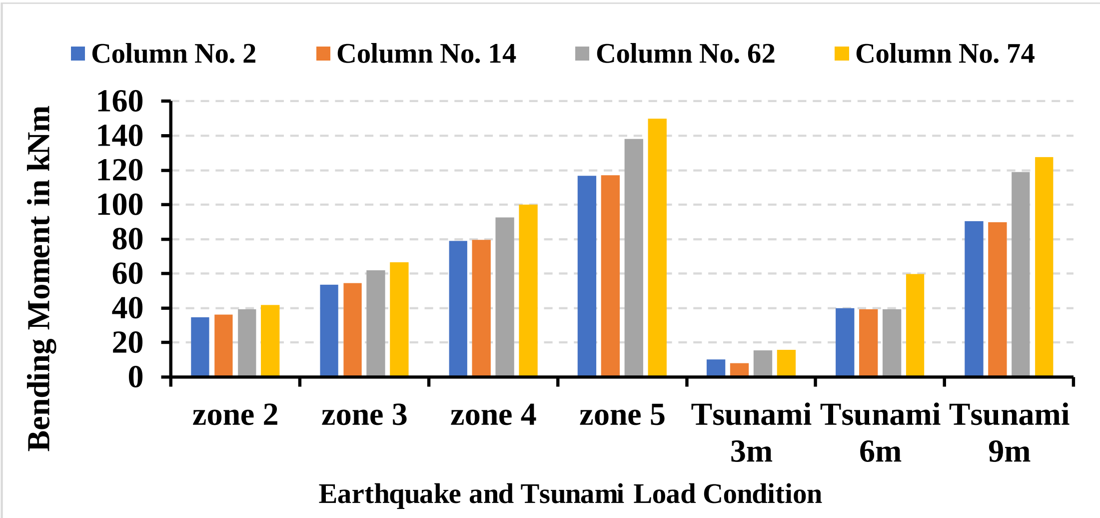

Fig. 21 Bending Moment in the columns due to earthquake and Tsunami loads for configuration 3

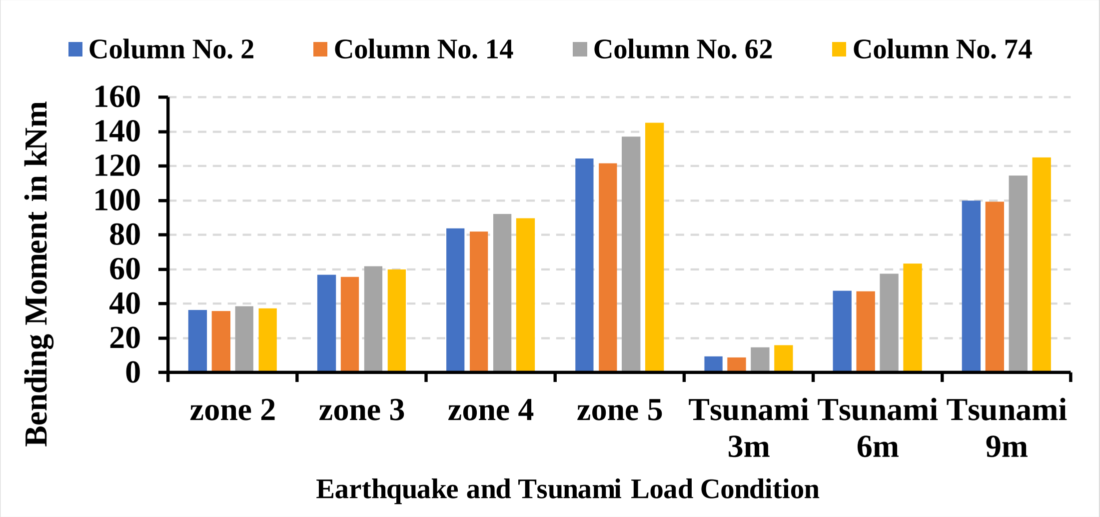

Fig. 22 Bending Moment in the columns due to earthquake and Tsunami loads for configuration 4

STOREY DISPLACEMENT AND STOREY DRIFT

In Figures 23, 24, 25, and 26, we provide a comprehensive visualization of the storey displacement and in Figure 27, 28, 29, and 30 we provide comprehensive visualization of storey drift resulting from both seismic and tsunami loads. When analyzing the response to earthquake forces, a consistent pattern becomes evident across all structural configurations. Specifically, in structural configuration 1, the inter-storey displacement between adjacent floors induced by seismic loading exhibits a relatively uniform distribution. However, in structural configurations with and without infill walls, this inter-storey displacement varies more significantly. Additionally, it's notable that the storey displacement due to earthquake forces is more or less proportional to the seismic mass of the structure at different levels.

The average story drift for zone 2 is 0.030%H for configuration 1, 0.031%H for configuration 2, 0.032%H for configuration 3, and 0.038%H for configuration 4. The average story drift for zone 3 is 0.045%H for configuration 1, 0.048%H for configuration 2, 0.049%H for configuration 3, and 0.058%H for configuration 4. The average story drift for zone 3 is 0.065%H for configuration 1, 0.07%H for configuration 2, 0.070%H for configuration 3, and 0.081%H for configuration 4. The average story drift for zone 4 is 0.093%H for configuration 1, 0.103%H for configuration 2, 0.0103%H for configuration 3, and 0.118%H for configuration 4. The maximum story drift is 0.001194 H for configuration 1, 0.001192 H for configuration 2, 0.0013 H for configuration 3, and 0.0013 H for configuration 4. It is important to note that all these calculated values fall comfortably within the limiting drift prescribed by IS 1893-Part 1, 2016 [14]. The allowable limits specified by the standard is 0.004 H [14]. The maximum storey drift for The maximum storey drift was observed at the elevation of 6 m above ground for all the earthquake zones.

Shifting our focus to the influence of tsunami forces on the structural response, we observe that the inter-storey displacement between adjacent floors is more pronounced below the tsunami inundation depth. In contrast, above the level of tsunami inundation depth, the storey displacement remains relatively uniform across all considered tsunami inundation depths. This phenomenon highlights the distinct behavior of the structure's response to tsunami forces, particularly in terms of inter-storey displacement, which is influenced by the depth of tsunami inundation. The maximum storey drift was observed at the elevation of 3 m above ground for all the tsunami heights.

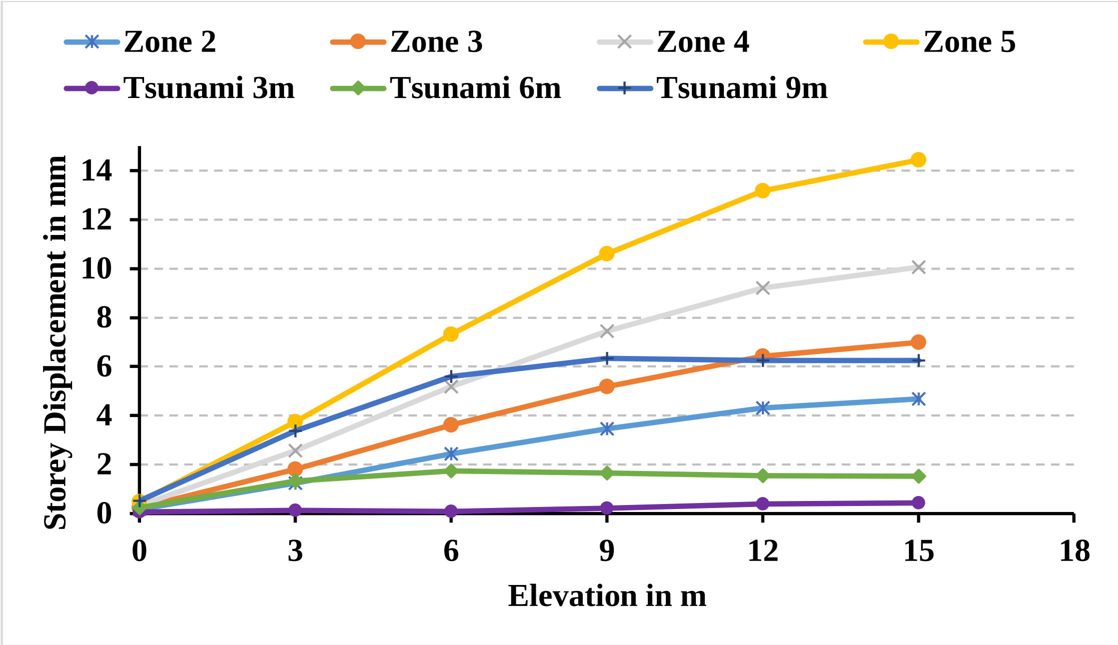

Fig. 23 Storey Displacement due to earthquake and Tsunami loads for configuration 1

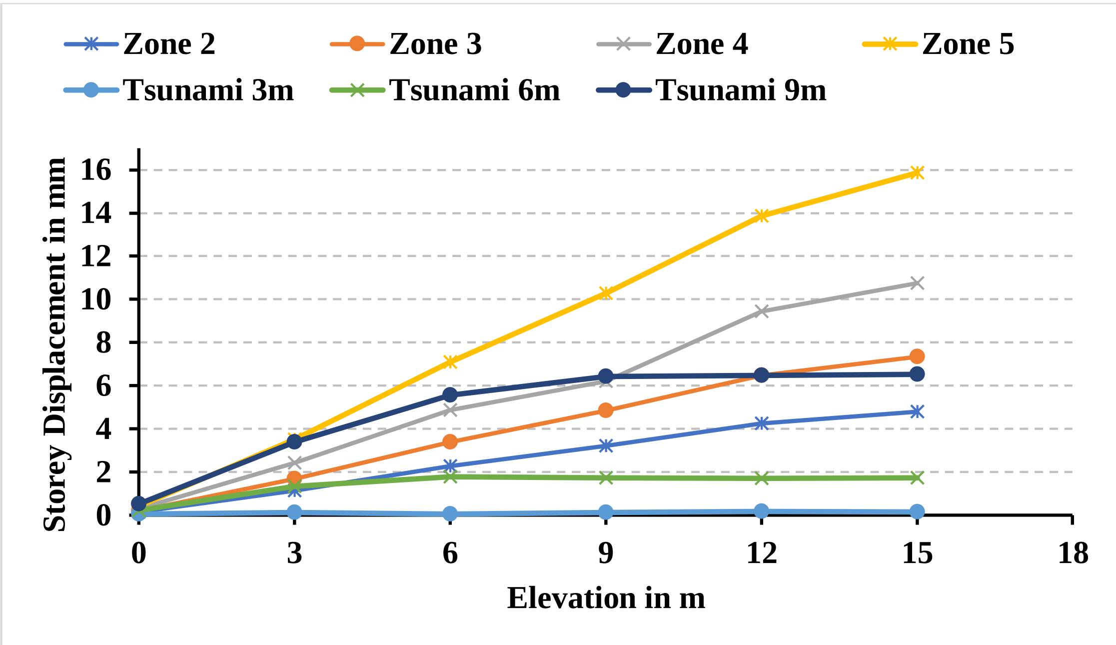

Fig. 24 Storey Displacement due to earthquake and Tsunami loads for configuration 2

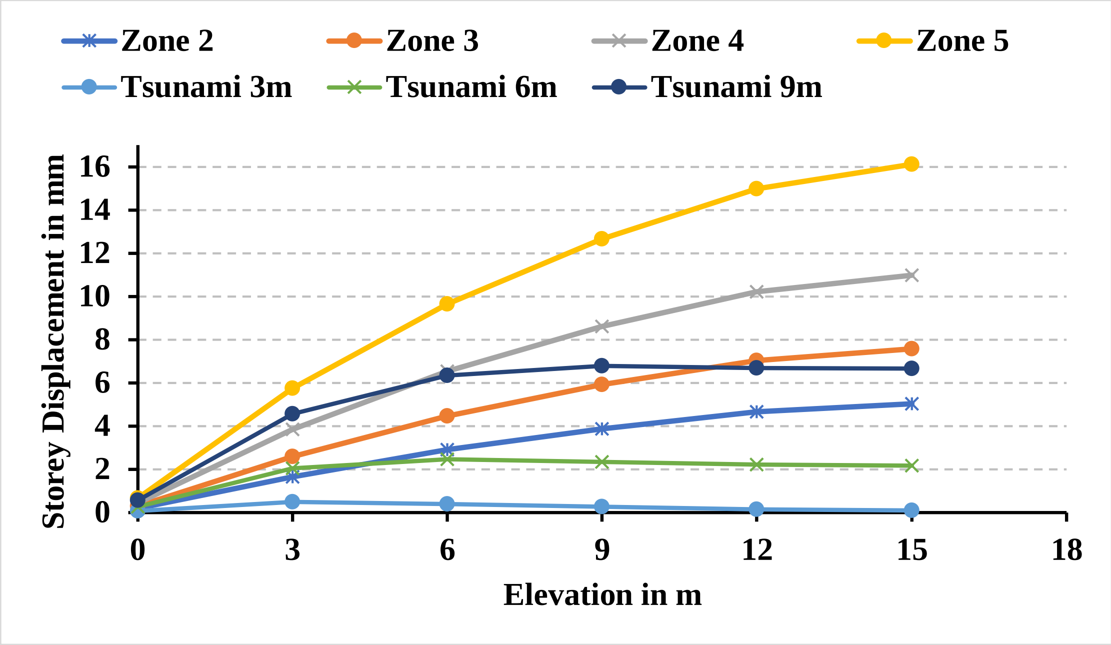

Fig. 25 Storey Displacement due to earthquake and Tsunami loads for configuration 3

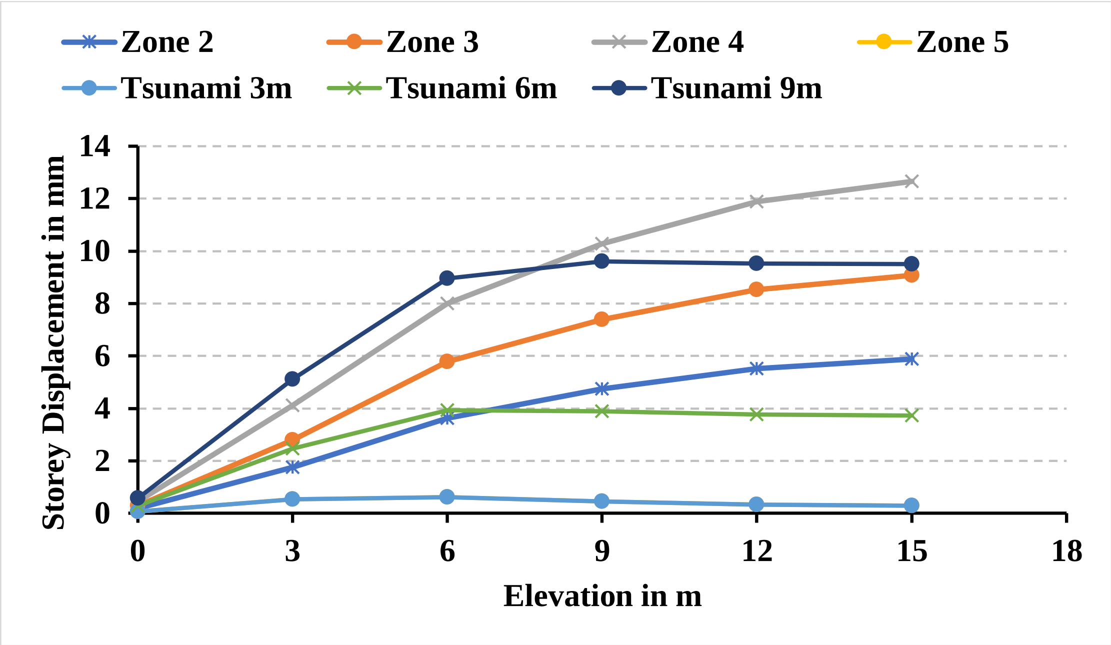

Fig. 26 Storey Displacement due to earthquake and Tsunami loads for configuration 4

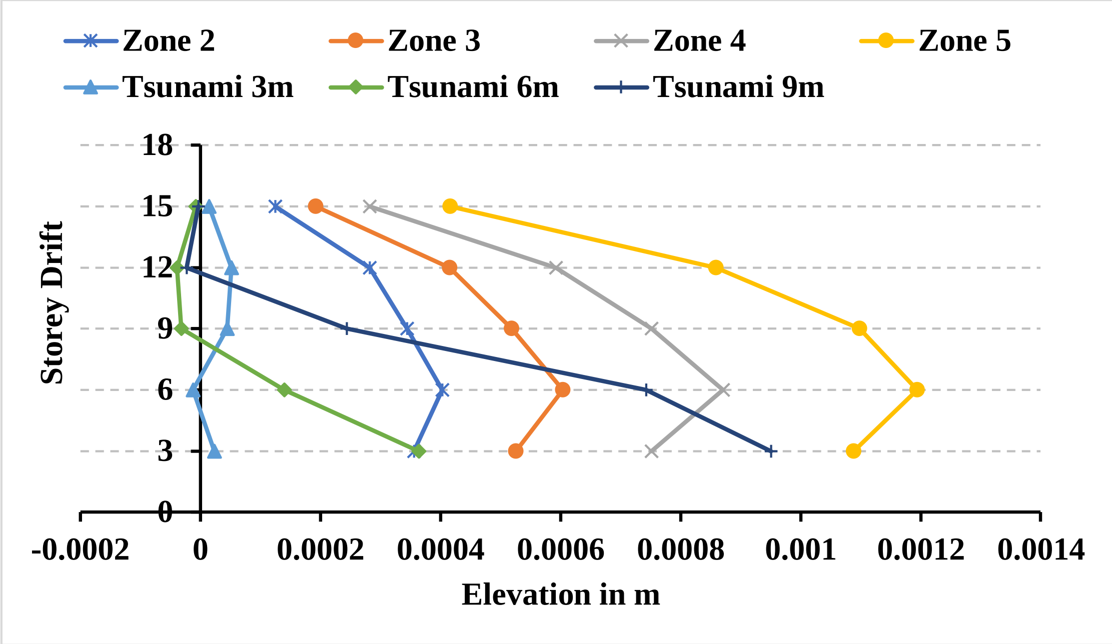

Fig. 27 Storey Drift due to earthquake and Tsunami loads for configuration 1

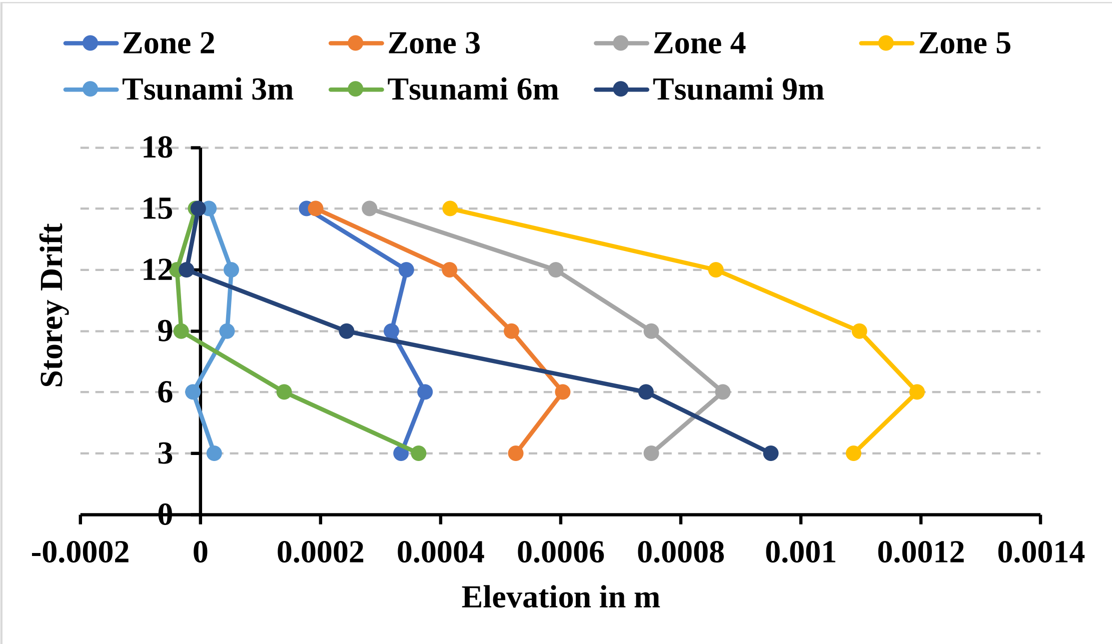

Fig. 28 Storey Drift due to earthquake and Tsunami loads for configuration 2

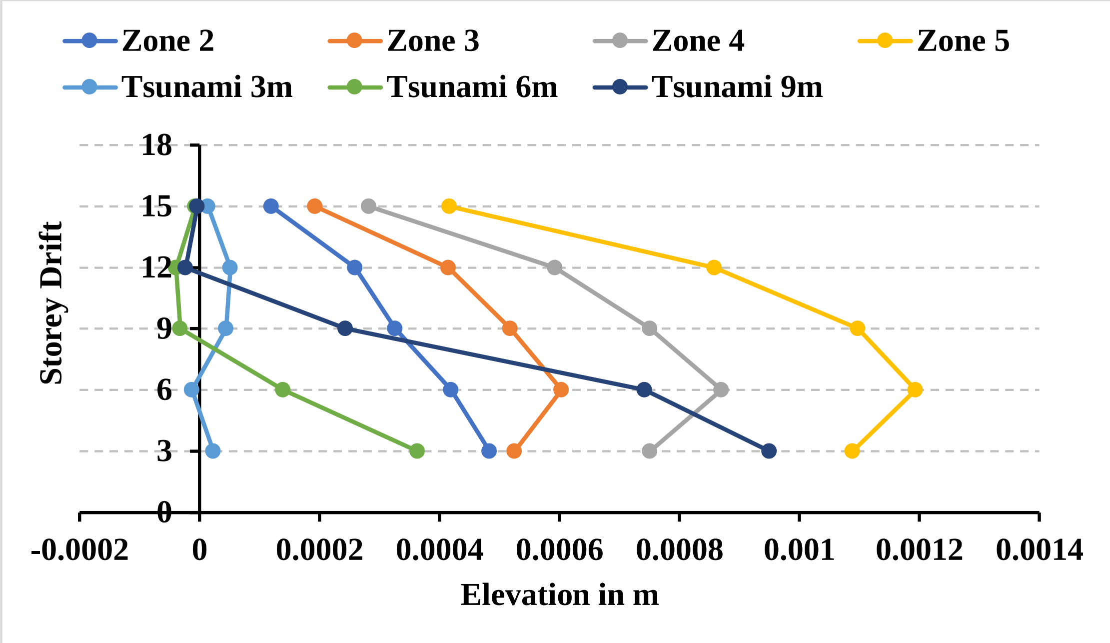

Fig. 29 Storey Drift due to earthquake and Tsunami loads for configuration 3

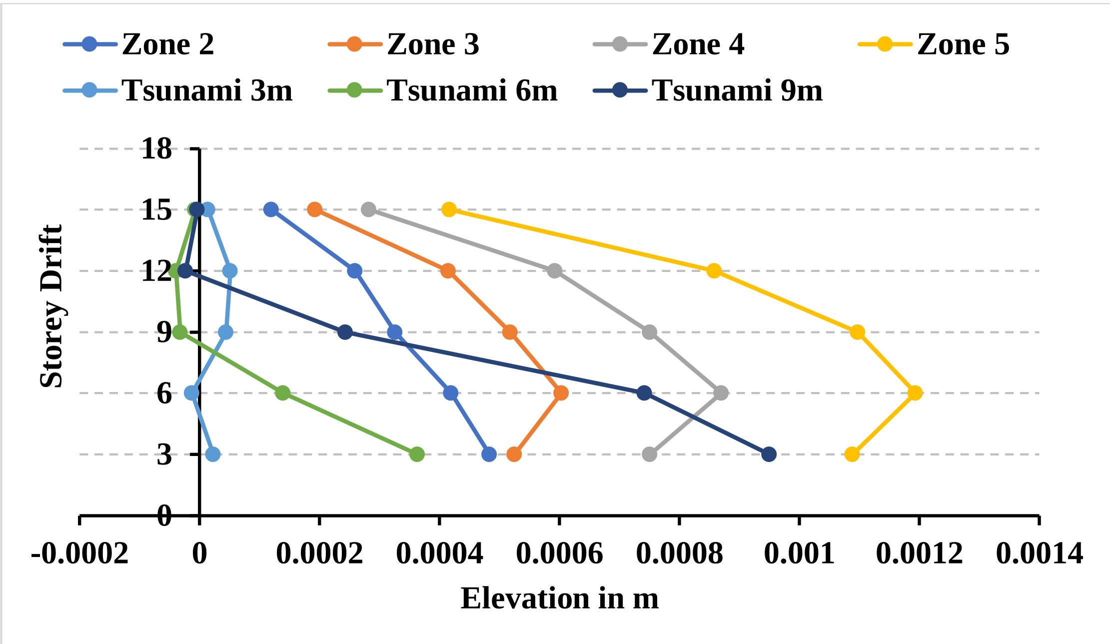

Fig. 30 Storey Drift due to earthquake and Tsunami loads for configuration 4

CONCLUSIONS

The study explores four distinct structural configurations and reveals the significant impact of architectural choices, such as the presence of infill walls, on structural responses to seismic and tsunami forces. These findings underline the need for meticulous design considerations in tsunami-prone areas. In light of the analysis conducted in this study, encompassing the response of reinforced concrete buildings to earthquake and tsunami forces, following findings emerge.

1. Earthquake and tsunami forces can lead to substantial lateral forces on a building's foundation, especially during high tsunami wave events. The study shows that structural configuration 1 and 2 consistently experiences the highest base shear due to its large frontal area exposed to tsunami waves which was around 18%, 20.5%, and 35.5% higher in comparison with Configuration 3 and 4 for the tsunami elevation of 3 m, 6 m, and 9 m respectively.

2. The columns at the forefront of the structure bear the brunt of tsunami impact, resulting in the highest axial and shear forces in the middle columns which was averagely 68% higher for exterior column and 160% higher for interior column. Understanding these forces' distribution is crucial for structural design and reinforcement in coastal regions.
3. Bending moments induced by seismic and tsunami loads demonstrate varying patterns. The presence or absence of infill walls in lower floors significantly influences the distribution of bending moments. This insight emphasizes the role of infill walls in governing structural behavior.
4. The study observes that storey drift is more pronounced below the tsunami inundation depth. Above this level, the storey displacement remains relatively uniform. However, for all the earthquake zones and tsunami inundation depth studies the storey drift values were well below 0.004 H limit prescribed by the Indian Standard.

REFERENCES

1. Demirel, I.O., Yakut, A. and Binici, B. (2022). "Seismic Performance of Mid-Rise Reinforced Concrete Buildings in Izmir Bayrakli after the 2020 Samos Earthquake", *Eng Fail Anal, Vol. 137, doi:10.1016/j.engfailanal.2022.106277*.
2. Sugawara, D. (2021). "Numerical Modeling of Tsunami: Advances and Future Challenges After the 2011 Tohoku Earthquake and Tsunami", *Earth-Science Reviews, Vol. 214. Elsevier B.V., doi:10.1016/j.earscirev.2020.103498*.
3. Cortez, C., Jünemann, R., Fernández, C., Urrutia, A., Crempien, J.G.F. and Cienfuegos, R. (2022). "Performance of an RC Building Under Seismic and Tsunami Actions in Sequence Via Nonlinear Dynamic Analysis Including Soil-Structure Interaction", *Eng Struct, Vol. 272, doi:10.1016/j.engstruct.2022.114942*.
4. Xiong, Y., Liang, Q., Park, H., Cox, D. and Wang, G. (2019). "A Deterministic Approach for Assessing Tsunami-Induced Building Damage Through Quantification of Hydrodynamic Forces", *Coastal Engineering, Vol. 144, pp. 1–14, doi: 10.1016/j.coastaleng.2018.11.002*.
5. Madurapperuma, M.A.K.M. and Wijeyewickrema, A.C. (2013). "Response of Reinforced Concrete Columns Impacted by Tsunami Dispersed 20' and 40' Shipping Containers", *Eng Struct, Vol. 56, pp. 1631–1644, doi: 10.1016/j.engstruct.2013.07.034*.
6. Maheshwari, B.K., Sharma, M.L. and Narayan, J.P. (2005). "Structural Damages on the Coast of Tamil Nadu Due to Tsunami Caused by December 26, 2004 Sumatra Earthquake", *[Online], Available:http://www.prh.noaa.gov/itic/.*
7. Puspito, N.T. and Gunawan, I. (2005). "Tsunami Sources in the Sumatra Region, Indonesia and Simulation of the 26 December 2004 Aceh Tsunami", *[Online], Available:http://www.pmel.noaa.gov/tsunami/research.html.*
8. Saatcioglu, M., Ghobarah, A. and Nistor I. (2005). "Effects of the December 26, 2004 Sumatra Earthquake and Tsunami on Physical Infrastructure", *[Online], Available: www.geocities.com*.
9. Fritz, H.M. and Borrero, J.C. (2006). "Somalia Field Survey after the December 2004 Indian Ocean Tsunami", *Earthquake Spectra, Vol. 22, No. 3_suppl, pp. 219–233, doi: 10.1193/1.2201972*.
10. Snigdha, S., Jaiswal, A., Gandhid, P. and Sheth. A. (2006). "Effects of the December 2004 Indian Ocean Tsunami on the Indian Mainland", *Earthquake Spectra, Vol. 22, No. S3, pp. S435–S473*.
11. Leelawat, N., Suppasri, A., Murao, O. and Imamura, F. (2016). "A Study on the Influential Factors on Building Damage in Sri Lanka During the 2004 Indian Ocean Tsunami", *Journal of Earthquake and Tsunami, Vol. 10, No. 2, doi: 10.1142/S1793431116400017*.
12. E.D.C. Headquarters and others (2013). "Damage Situation and Police Countermeasures Associated with 2011 Tohoku District–Off the Pacific Ocean Earthquake", *Tokyo: National Police Agency of Japan*.
13. Kodanda, P., Rao, R. and Reddy, S.R.K. (2010). "Response of Coastal Buildings Subjected to Seismic and Tsunami Forces".
14. BIS: 1893-Part1 (2016). "Criteria for Earthquake Resistant Design of Structures Part 1 General Provisions and Buildings (Sixth Revision)", *[Online], Available: www.standardsbis.in.*
15. FEMA 55 (2011). "Coastal Construction Manual Principles and Practices of Planning, Siting, Designing, Constructing, and Maintaining Residential Buildings in Coastal Areas (Fourth Edition) - Volume I".

16. FEMA 55 (2011). “Coastal Construction Manual: Principles and Practices of Planning, Siting, Designing, Constructing, and Maintaining Residential Buildings in Coastal Areas (Fourth Edition) - Volume II”.
17. FEMA P646 (2019). “Guidelines for Design of Structures for Vertical Evacuation from Tsunamis Third Edition”, *[Online], Available: www.ATCouncil.org.*
18. Lukkunaprasit, P., A. Ruangrassamee, and N. Thanasisathit. (2009). “Tsunami Loading on Buildings with Openings”, *Science of Tsunami Hazards*, Vol. 28, No. 5, pp. 303–310.
19. Ghobarah, A., Saatcioglu, M. and Nistor, I. (2006). “The Impact of the 26 December 2004 Earthquake and Tsunami on Structures and Infrastructure”, *Eng Struct, Vol. 28, No. 2, pp. 312–326, doi:10.1016/j.engstruct.2005.09.028*.
20. Kihara, N. *et al.* (2021). “A Physical Model of Tsunami Inundation and Wave Pressures for an Idealized Coastal Industrial Site”, *Coastal Engineering, Vol. 169, doi: 10.1016/j.coastaleng.2021.103970*.
21. Latcharote, P. and Kai, Y. (2014), “Nonlinear Structural Analysis of Reinforced Concrete Buildings Suffering Damage From Earthquake and Subsequent Tsunami”, Tenth U.S. National Conference on Earthquake Engineering, Frontiers of Earthquake Engineering, July 21-25, 2014, Anchorage, Alaska.
22. Petrone, C., Rossetto, T., Baiguera, M., De la Barra Bustamante, C. and Ioannou, I. (2020). “Fragility Functions for a Reinforced Concrete Structure Subjected to Earthquake and Tsunami in Sequence”, *Eng Struct*, Vol. 205, doi: 10.1016/j.engstruct.2019.110120.
23. Tagle, S.J., Jünemann, R., Vásquez, J., de la Llera, J.C. and Baiguera, M. (2021). “Performance of a Reinforced Concrete Wall Building Subjected to Sequential Earthquake and Tsunami Loading”, *Eng Struct, Vol. 238, doi: 10.1016/j.engstruct.2021.111995*.
24. Rossetto, T., De la Barra, C., Petrone, C., De la Llera, J.C., Vásquez, J. and Baiguera, M. (2019). “Comparative Assessment of Nonlinear Static and Dynamic Methods for Analysing Building Response under Sequential Earthquake and Tsunami”, *Earthq Eng Struct Dyn, Vol. 48, No. 8, pp. 867–887, doi:10.1002/eqe.3167*.
25. Rossetto, T., Petrone, C., Eames, I., De La Barra, C., Foster, A. and Macabuag, J. (2018). “Advances in the Assessment of Buildings Subjected to Earthquakes and Tsunami”, *Geotechnical, Geological and Earthquake Engineering, Springer Netherlands, pp. 545–562. doi: 10.1007/978-3-319-75741-4_23*.
26. Cortez, C., Jünemann, R., Fernández, C., Urrutia, A., Crempien, J.G.F. and Cienfuegos, R. (2022). “Performance of an RC Building under Seismic and Tsunami Actions in Sequence Via Nonlinear Dynamic Analysis Including Soil-Structure Interaction”, *Eng Struct, Vol. 272, doi:10.1016/j.engstruct.2022.114942*.
27. Palermo. D and Nistor. I. (2008). “Understanding Tsunami Risk to Structures: A Canadian Perspective”, *Science of Tsunami Hazards, Vol. 27, No. 4*.
28. Sutarja, N., Pringgana, G. and Wikrama, M.A.S. (2021). “The Effects of Earthquake and Tsunami Loadings on Structural Behavior of Reinforced Concrete Building”, *Journal of Applied Engineering Science, Vol. 19, No. 2, pp. 282–291, doi: 10.5937/jaes0-25655*.